Liquid Crystals
Publication details, including instructions for authors and subscription information:
http://www.informaworld.com/smpp/title~content=t713926090

A mesoscale modelling study of nematic liquid crystals confined to ellipsoidal domains

Rishikesh K. Bharadwaj; Timothy J. Bunning; B. L. Farmer

Online publication date: 06 August 2010

To cite this Article Bharadwaj, Rishikesh K. , Bunning, Timothy J. and Farmer, B. L.(2000) 'A mesoscale modelling study of nematic liquid crystals confined to ellipsoidal domains', Liquid Crystals, 27: 5, 591 — 603
To link to this Article: DOI: 10.1080/026782900202435
URL: http://dx.doi.org/10.1080/026782900202435

LIQUID CRYSTALS, 2000, VOL. 27, NO. 5, 591–603

A mesoscale modelling study of nematic liquid crystals confined to ellipsoidal domains

RISHIKESH K. BHARADWAJ
Systran Federal Corporation, Dayton, OH 45431-1672, USA

TIMOTHY J. BUNNING
Air Force Research Laboratory,
Materials and Manufacturing Directorate (AFRL/MLPJ) WPAFB,
OH 45433-7702, USA

B. L. FARMER*
Air Force Research Laboratory,
Materials and Manufacturing Directorate (AFRL/MLBP), 2941 P Street, Ste 1,
WPAFB, OH 45433-7750, USA

(*Received 2 August 1999; accepted 11 November 1999*)

Director configurations of nematic liquid crystalline molecules packed in ellipsoidal domains have been investigated using mesoscale modelling techniques. Interactions between the directors were described by the Lebwohl–Lasher potential. Four different ellipsoidal shapes (sphere, oblate spheroid, prolate spheroid, and ellipsoid) were studied under homogeneous and homeotropic surface anchoring conditions. The model has been characterized by computing thermodynamic and structural properties as a function of ellipsoidal shape (prolate and oblate) and size. The predicted director configuration in ellipsoids resulting from homeotropic surface anchoring is found to be very different from that in spherical domains. The bipolar configuration involving homogeneous surface anchoring is nearly identical in the four cases. The effect of an external electric field, applied at different orientations with respect to the major axis of the ellipsoid, has been probed as a function of the magnitude of the field and the ellipsoidal size and shape. The orientation of directors is most easily accomplished parallel and perpendicular to the major axis for the oblate and prolate spheroids, respectively, for homeotropic anchoring, and along the bipolar symmetry axis for homogeneous anchoring. In domains with homeotropic surface anchoring, the oblate spheroid and elongated ellipsoid are predicted to be the most efficient geometries for PDLC applications; for homogeneous anchoring conditions, the prolate spheroid and elongated ellipsoid are predicted to be the most efficient.

1. Introduction

The study of nematic liquid crystalline molecules confined to sub-micrometer size domains, as encountered in polymer dispersed liquid crystals (PDLCs) [1, 2], has provoked a great deal of fundamental research. The effect of confinement on the thermodynamics of liquid crystalline organization is a topic of current interest, fuelled in no small part by the tremendous potential technological impact of such materials. An enduring question in the area of PDLCs is the nature of the relationship between the domain geometry (shape and size) and the resulting electro-optical properties. In particular, PDLC materials possessing domains with ellipsoidal geometry have attracted much interest. The optical contrast ratio of PDLC films is larger for domains possessing ellipsoidal geometry than for those with spherical geometry [3]. Our interest stems from electrically switchable holographic transmission gratings where sub-micrometer sized domains possessing ellipsoidal geometry are almost exclusively observed [4–8]. The anisotropic shape inherent in these systems is due to non-uniform elastic deformation of the domains upon phase separation. Local differences in the crosslink density of the polymer matrix induces anisotropic stresses on the domains. This anisotropy is particularly acute when the Bragg spacing decreases. Thus, reflection gratings which have periodicities on the order of 100–2200 nm

*Author for correspondence; e-mail: barry.farmer@afrl.af.mil

Liquid Crystals ISSN 0267-8292 print/ISSN 1366-5855 online © 2000 Taylor & Francis Ltd
http://www.tandf.co.uk/journals

almost exclusively exhibit non-spherical domains. Such gratings possess many attractive properties such as a high diffraction efficiency, low switching voltages (~ 5 V μm^{-1}) and extremely rapid response times (microseconds) due to the small domain sizes.

Electric fields are commonly used to elicit the desired response from PDLC materials. Upon application of an external field, the directors orient themselves along the direction of the field (for positive dielectric anisotropy LCs) and thereby render the PDLC transparent. The original director configuration, determined by the surface anchoring and the droplet shape, is regained upon removal of the field. Anisotropy and the varying curvature associated with ellipsoidal shapes complicates the response of the directors to an applied field, depending on the orientation of the field with respect to the axes of the ellipsoid. This results in the electric field inside the domain, although uniform, to be pointed along a different direction compared with the applied field [9, 10] depending on the extent of mismatch in refractive indices of the polymer and liquid crystalline phases. The response of a PDLC, consisting of a large number of such domains, will therefore be an average over all orientations of the domains with respect to the applied field. Studies have shown that the response times and switching voltages are a function of aspect ratio, as well as of the shape of the elongated domains [10]. However, interpretation of experimental results is often complicated by the fact that both the nature of the polymeric matrix and the domain size can play important roles in determining the switching voltage and response times.

Experimental data show the behaviour of anisotropic domain shapes to be different from and in fact more efficient than that of spherical domains. There remains a need for a thorough investigation of the influence of domain size and shape effects on the director configuration and response to an applied field. We have therefore chosen computer simulations to carry out a systematic investigation of well defined systems. At the heart of the simulation method adopted here is the fact that many properties of liquid crystalline molecules may be predicted with remarkable accuracy using an interaction potential that is a function only of the relative director orientation. Using such a potential in conjunction with Monte Carlo sampling [11], Lebwohl and Lasher [12] were able to reproduce the nematic to isotropic transition for a lattice of vectors under periodic boundary conditions. A large number of such 'mesoscale' computer simulation studies have been performed on a variety of systems. These studies include the prediction of thermodynamic, structural and morphological properties of nematics in the bulk [12–14], in isolated spherical [15–19] and cylindrical [20, 21] domains, in aerogels [22, 23], at the polymer–liquid crystalline interfaces [24], and in polymeric liquid crystals [25, 26]. With particular relevance to the PDLC case, extensive simulations of nematic liquid crystals confined to spherical domains with radial [15, 16], toroidal [17], and bipolar [18] configurations have been performed. In general the molecular organization and response to applied fields [27, 28] are very well understood in the case of spherical domains.

Admittedly, the 'coarse-grained' approach does not come without certain sacrifices. Since there is no concept of time in the simulations, only equilibrium properties may be studied. Therefore, dynamic quantities such as response times that could be directly compared with experimental data cannot be obtained. Neglect of viscous and diffusive effects in the model would also need to be considered when results are compared with experiment. In addition, direct comparisons with experimental results are hampered by the fact that simulations pertain to single isolated domains [29] and neglect to incorporate the effect of the surrounding polymeric matrix directly. Despite these drawbacks the mesoscale method has proven to be of immense value in addressing a wide range of phenomena that are currently out of bounds to atomistic approaches. The principal focus of the present work is the systematic study of the equilibrium director configuration of nematic liquid crystals within ellipsoidal droplets, with both homeotropic and homogeneous surface anchoring and as a function of domain size and shape, and its response to an applied field.

2. Simulation details

The model consists of an array of unit vectors defining the nematic liquid crystal director ($\mathbf{n}_i$) placed on a simple cubic lattice. An ellipsoidal cluster of directors is created from a cubic lattice by selectively deleting vectors to yield the desired geometry and size defined by the a, b and c dimensions of the ellipsoid given in terms of the number of cells. Four different types of domain shape were studied; spherical ($a = b = c$), oblate spheroid ($a < b = c$), prolate spheroid ($a > b = c$), and ellipsoid ($a \neq b \neq c$). In each case different domain sizes were studied. In studies involving homeotropic surface anchoring, the initial configuration was constructed by defining vectors normal to the surface for each successive ellipsoidal layer. In the case of a sphere, a perfect radial configuration is obtained, while the configuration is 'radial-like' in the case of the ellipsoids due to the varying surface curvature. In all cases involving the radial configuration a centrally located point defect (hedgehog) was present. A similar approach was used to construct domains with bipolar configuration involving homogeneous surface anchoring, by defining a bipolar symmetry axis and constructing the vectors tangential to the surface. In this case two surface defects (boojums) were located at antipodal points of the

bipolar symmetry axis. In the case of prolate spheroids and ellipsoids the major axis (a) was chosen as the bipolar symmetry axis, whereas for the oblate spheroids the bipolar symmetry axis was defined in the bc plane, along the b axis. Of course, in the spherical case all definitions of the bipolar axis are equivalent due to symmetry. Two types of vector are defined; vectors on the surface defining the boundary of the domain with their orientation fixed throughout the simulation, and vectors lying within the domain that are capable of changing orientation. The surface vectors were held fixed in either the homeotropic or homogeneous anchoring condition throughout the simulation.

The directors defining the local orientation of the liquid crystal interact via the Lebwohl–Lasher [12] potential such that a given director interacts only with its six nearest neighbours through the following expression

$$U_{ij} = \sum_{j=1}^{6} \frac{\varepsilon_{ij}}{2}(1 - 3|\mathbf{n}_i \ \ \mathbf{n}_j|^2) \tag{1}$$

where U_{ij} is the potential energy of interaction, ε_{ij} is a positive constant (ε, for nearest neighbours and zero for otherwise), and $\mathbf{n}_i$ and $\mathbf{n}_j$ are unit vectors corresponding to the liquid crystal director under consideration and its six surrounding nearest neighbours, respectively. In simulations involving an externally applied field, an additional term was added to the potential energy expression with the same functional form as in equation (1) given by

$$U_E = \frac{E}{2}(1 - 3|\mathbf{n}_i \ \ \mathbf{n}_E|^2) \tag{2}$$

where $\mathbf{n}_E$ is a unit vector representing the direction of an applied field of strength E. The average energy for the array of directors in dimensionless units is given by

$$U^* = \frac{1}{N\varepsilon} \sum_{i=1}^{N} U_{ij}. \tag{3}$$

With the interaction potential and the ellipsoidal domain defined, a Monte Carlo procedure is invoked to explore phase space. The standard Metropolis algorithm has been followed [11]. Briefly, a director is selected at random from the array and its energy computed according to equation (1). The orientation of the director is then altered and the energy is computed again. If the energy of the trial orientation is lower than that of the initial orientation the move is accepted. When the energy of the trial orientation is higher than that of the initial orientation, the trial orientation is accepted with a probability given by

$$p = \exp\left(-\frac{U_{\text{trial}} - U_{\text{initial}}}{kT}\right) \tag{4}$$

where k is the Boltzmann constant and T is the temperature. Therefore thermal effects are introduced indirectly through the sampling and a reduced temperature may be defined as $T^* = kT/\varepsilon_{ij}$. Thus, the effect of temperature on the director configuration and thermodynamic properties such as those accompanying the nematic to isotropic transition may be examined.

At this stage it is appropriate to comment on the choice of the trial orientation. In general, as equilibrium is approached fewer trial orientations are accepted and consequently the simulation becomes extremely inefficient. The acceptance ratio, the ratio of successful trial moves to the total number of attempts, becomes very small. An acceptance ratio of 0.5, which is almost universally chosen in Monte Carlo studies, has been used here [30]. Maintaining this value requires a restriction on the extent of angular variation of the trial orientation from the initial orientation. The trial orientation is chosen from within a cone of semi-angle δ defined around the initial director orientation. By varying the semi-angle it is possible to maintain an acceptance ratio of 0.5. In practice, the semi-angle of the cone was monitored during the course of the simulation and redefined every 500 Monte Carlo cycles by weighting it with the ratio of the acceptance ratio calculated over that period to the required acceptance ratio (0.5).

Several different reduced temperatures were studied in the range 0.05 to 1.55 in steps of 0.05 units. A perfect radial configuration in the case of the spherical domain, or radial-like configuration in the case of ellipsoidal domains, were used as the initial orientation. All systems studied achieved equilibrium, judged by monitoring the system energy, within 1000 iterations. Properties of interest were averaged over the last 8000 iterations of a total of 10 000 iterations. The number of Monte Carlo cycles is given by the product of the number of movable vectors involved in the simulation and the total number of iterations. In simulations involving an externally applied field, several different values of the applied field were studied in the range 0.05 to 2.0 reduced units.

The program used in this study was originally developed by Windle and co-workers [25, 26] and has been suitably modified for the purposes here. All computations were performed on a dual processor R10000/225MHz Silicon Graphics OCTANE2 workstation.

3. Results and discussion

3.1. *Equilibrium properties*

We begin by characterizing the model by computing the dimensionless heat capacity C^*. Differentiation of the average dimensionless potential energy U^* with respect to temperature yields the heat capacity. In addition the structure was analysed by computing the order parameter. The order parameter was defined by the largest

positive eigenvalue S_λ resulting from the diagonalization of the order tensor **S** given by [13, 29]

$$\mathbf{S} = \frac{1}{N}\sum_{i=1}^{N}\frac{1}{2}(3\mathbf{n}_{i\alpha}\mathbf{n}_{i\beta} - \delta_{\alpha\beta}) \tag{5}$$

where $\mathbf{n}_i$ represents the director orientation and $\delta_{\alpha\beta}$ is the unit tensor. The eigenvector corresponding to the largest positive eigenvalue represents the instantaneous director $\mathbf{n}_\lambda$ of the assembly. The director evolves in spatial orientation as the simulation proceeds. Therefore this quantity captures rigorously any order that may be present in the system without the need for an *a priori* guess for the sample director. The eigenvalues can have a value between 1, indicating parallel alignment, and -0.5 indicating perpendicular alignment, with a value of zero indicating random order. These quantities have been used previously with success in studying similar systems such as in the simulations of liquid crystals confined to spherical domains [15–18] and in the simulation of bulk systems with periodic boundary conditions [12, 13]. Therefore the computation of these quantities constitutes an important calibration step for the model and simulation methods used in this study.

The temperature dependence of C^* and S_λ are shown in figures 1 and 2 for oblate and prolate spheroids respectively under both homeotropic (radial) and homogeneous (bipolar) surface alignments. In the case of spheroidal and ellipsoidal geometries, all orientations of the bipolar symmetry axis are not equal in energy. The symmetry axis tends to align along the longest distance available in the domain. For oblate spheroids the symmetry axis lies in the plane defined by the two minor axes (*bc* plane), while in the prolate and ellipsoidal domains the symmetry axis lies along the major (*a*) axis. In each case the 'prolateness' and 'oblateness' of the domains was varied until they culminated in a spherical domain with a diameter of 19 lattice cells (3887 vectors). This gives rise to prolate and oblate domains with the number of directors (volume) gradually increasing as the spherical geometry is attained. In addition, ellipsoidal ($a \neq b \neq c$) domains of different sizes were also studied. In general, the peak in C^* increases in height as the size of the domain is increased and is higher for the bipolar domains compared with the radial domains of the same size. In prolate spheroids with the bipolar configuration (symmetry axis along *a*), the peaks are more well defined

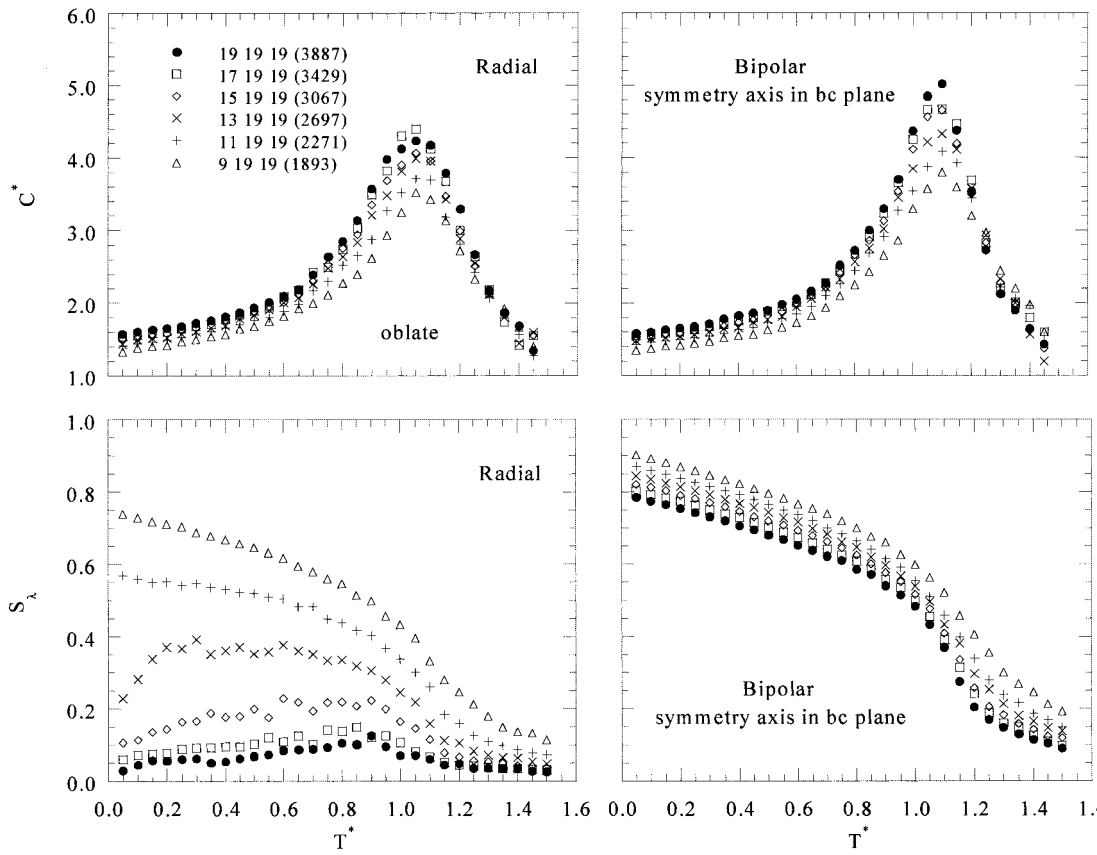

Figure 1. Temperature dependence of the dimensionless heat capacity (C^*) and the order parameter (S_λ) for oblate spheroids of different sizes for both homeotropic and homogenous surface anchoring conditions. The dimensions are given in terms of the number of lattice cells and the total number of vectors constituting the domain.

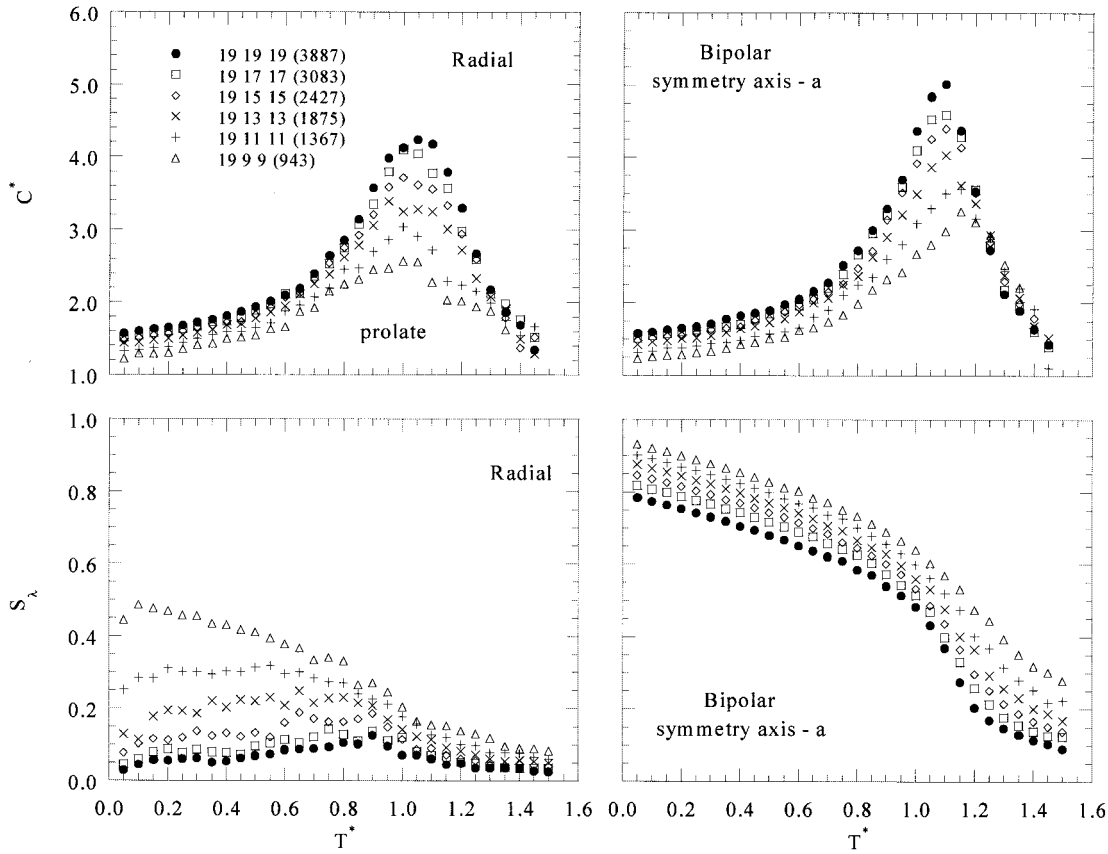

Figure 2. Temperature dependence of the dimensionless heat capacity (C^*) and the order parameter (S_λ) for prolate spheroids of different sizes for both homeotropic and homogenous surface anchoring conditions. The dimensions are given in terms of the number of lattice cells and the total number of vectors constituting the domain.

and shifted appreciably to higher T^* values as the prolateness is increased compared with the radial configuration. This indicates that the parallel director alignment encountered in bipolar droplets is more stable compared with the radial configuration. A similar trend was obtained with ellipsodal domains (not shown). These results are similar to those obtained with previous simulations of spherical droplets with a variety of different configurations (radial, toroidal, bipolar) [18] using the Lebwohl–Lasher potential. All showed a similar peak in the heat capacity, the height (C^*_{max}) and position (T^*_{max}) of which increased with increasing droplet size. For the spherical case, the maximum in the heat capacity occurs at the reduced temperatures T^*_{max} of 1.05 and 1.1, with C^*_{max} of 4.5 and 5.0 for the radial and bipolar configurations respectively. In addition, simulations of spheroidal and ellipsoidal domains with the bipolar symmetry axis defined to lie along the shortest distance available in the domain were performed. Accordingly, the symmetry axis lies along the a axis for oblate spheroids and in the bc plane for the prolate spheroids. In this case the T^*_{max} and C^*_{max} were found to be shifted towards lower values compared with those obtained with the former definition (symmetry axis along longest dimension) when compared on the basis of equal size and shape (not shown). In addition, U^* was displaced to higher values for the shortest dimension definition, indicating conclusively that the definition of the bipolar axis along the longest dimension was preferred.

It is worth mentioning that the behaviour observed here is a rather weak manifestation of the nematic to isotropic phase transition seen in bulk simulations ($30 \times 30 \times 30$ lattice) with periodic boundary conditions [13] using the Lebwohl–Lasher [12] potential, where C^*_{max} was found to be ~ 25 with T^*_{max} of 1.1232. Furthermore, the peak in the heat capacity was found to be extremely sharp and well defined, accompanied by an abrupt transition in the order parameter, with the transition being unequivocally identified as that of the first order. Clearly, the behaviour manifested here with a finite isolated domain is very different from that seen in the bulk with periodic boundaries. However, the results from the simulations are in direct agreement with experimental data [31–33] which also show the attenuation

of the nematic to isotropic transition upon the confinement of liquid crystalline phase. Therefore we classify the transition seen in this work as *pseudo* first order.

The temperature dependence of S_λ is shown in figures 1 and 2 for oblate and prolate domains with homeotropic and homogeneous surface anchoring. The results for homeotropic surface anchoring are discussed first. In the temperature dependence of S_λ, the classic order–disorder transition behaviour may be ascertained with decreasing domain sizes for both oblate and prolate spheroids. As the domain approaches spherical geometry, S_λ becomes increasingly noisy and approaches zero over the entire temperature range with a small anomaly in the vicinity of the peak observed in C^*. For a perfect radial configuration as in the case of a sphere, the system has no tendency to orient along any particular direction and this is reflected in the S_λ values which are very close to zero over the entire temperature range. This indicates the existence of the radial configuration within the spherical domain. As the spheroids become increasingly prolate or oblate, the departure from radial configuration also increases along with the establishment of a preferred direction of orientation which is seen in the S_λ dependence. This suggests that homeotropic surface anchoring produces markedly different director configurations within ellipsoidal domains.

For homogeneous surface anchoring, S_λ shows extremely well defined order–disorder behaviour as a function of temperature for all domains. This is expected since the bipolar configuration results in domains with a direction of preferred orientation that lies along the bipolar symmetry axis. As the oblateness or prolateness is increased, S_λ is shifted towards higher values indicating that parallel alignment of the directors is enhanced over the entire temperature range in bipolar domains. The exactly opposite behaviour is obtained when the bipolar symmetry axis is defined along the shortest dimension of the domain. In this case the effect of surface curvature on the director organization is very severe as the prolateness or oblateness is increased as expected from purely geometric considerations. This results in a weaker preference for the bipolar symmetry axis and therefore S_λ decreases in magnitude.

In order to probe the influence of ellipsoidal shape on the thermodynamic properties, it is necessary to construct the different shapes (spherical, prolate spheroidal, oblate spheroidal, ellipsoidal) such that the overall number of vectors (volume) is the same in each case. In this way the variations in the heat capacity or the order parameter may be correlated with shape effects alone. This was achieved by choosing a size for the spherical droplet and then building the other three shapes by trial and error to have approximately the same number of vectors. The results of such a comparison are shown in figure 3. The behaviour of C^* as a function of temperature is nearly identical for the four shapes suggesting that domain shape has a negligible effect on these properties. C^*_{max} for bipolar configuration is higher compared with the radial configuration for all shapes as seen previously. However, very marked differences may be seen in the behaviour of S_λ with temperature. For domains with the radial configuration (homeotropic anchoring) the order–disorder behaviour of S_λ becomes more pronounced as the geometry is varied from spherical → prolate spheroid → oblate spheroid and ellipsoid. This suggests that the director configuration within ellipsoidal domains is markedly different from the radial configuration observed in spherical domains. However, for domains with bipolar configuration, the order–disorder behaviour is well defined for all shapes with S_λ displaced toward higher values as the geometry is varied from spherical → oblate spheroid → prolate spheroid and ellipsoid. Furthermore, the temperature dependence of S_λ is nearly identical for the ellipsoidal and the prolate spheroidal geometries indicating that the director configuration is also similar in these two cases. The anisotropy associated with ellipsoidal (oblate spheroid, prolate spheroid, and ellipsoid) domains results in an inherent direction of preferred orientation for the bipolar symmetry axis that is absent in spherical domains.

3.2. *Director organization*

The observations made in the previous section are further substantiated by visual inspection of the equilibrated director configurations at $T^* = 0.2$ for the four cases (sphere, oblate spheroid, prolate spheroid, ellipsoid) shown in figures 4(*a–d*). In figure 4(*a*), the equilibrium director configurations under homeotropic and homogeneous surface anchoring conditions are shown for the spherical domain in the *bc* cross-section. The radial configuration is obtained under homeotropic surface anchoring conditions. Analysis of the two other cross-sections (*ab* and *ca*) confirmed this observation. In the *bc* cross-section, for the spherical domain with homogeneous surface anchoring, a bipolar configuration with the symmetry axis along the *b* axis may be discerned. The director field is strongly aligned along the symmetry axis with the two surface point defects (boojums) located at antipodal points of the bipolar axis.

Varying the surface curvature forces a distinctly different director configuration in the case of the ellipsoidal geometry, as seen in figures 4(*b–d*). The effect of anisotropy is most readily seen in the case of domains with homeotropic surface anchoring. We discuss the director configuration resulting from homeotropic surface anchoring first. For the oblate case shown in figure 4(*b*) the director organization may be best described as axial-like possessing an equatorial (*bc* plane) line defect lying

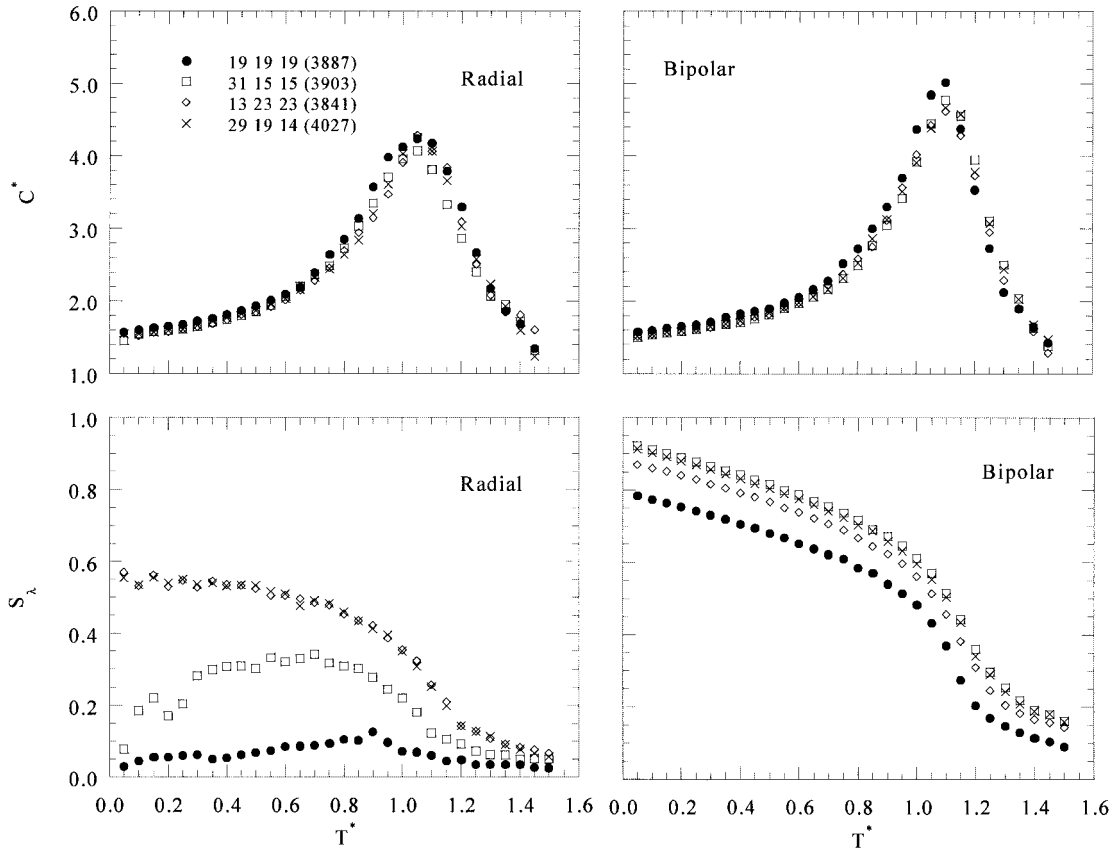

Figure 3. Comparison of the temperature dependence of C^* and S_λ for a spherical ($a = b = c$), oblate ($a < b = c$), prolate ($a > b = c$) spheroid, and ellipsoidal ($a \neq b \neq c$) domains with approximately the same number of directors in each case. The dimensions and the total number of directors are denoted for each geometry. The results for both homeotropic and homogeneous surface anchoring conditions are shown.

perpendicular to the direction of preferred orientation (*a* axis). This structure resembles the axial configuration with a line defect observed in spherical domains with radial configuration exposed to high electric or magnetic fields, as well as in systems with weak surface anchoring. However, the *encircling* equatorial line disclination is very pronounced and in fact extends well into the spheroid in the present case. The observation of an axial configuration in the case of oblate spheroids is easily understood by geometrical considerations. An oblate spheroid most closely resembles a flattened sphere, and for homeotropic surface anchoring a direction of preferred orientation is already present which lies along the direction in which the sphere was flattened. Furthermore, this result is expected to hold true regardless of the strength of the surface anchoring since the surface curvature already plays a very important part in stabilizing the axial configuration. Therefore the presence of an oblate spheroidal geometry may be added to the two well known conditions (strong fields and weak anchoring) under which the axial configuration is observed.

Prolate spheroids consist of two distinct geometrical attributes, a cylinder-like region in the middle of the spheroid where the surface curvature is very small, end-capped by two nearly hemispherical regions where the curvature is very large. Therefore it is reasonable to expect two distinct director configurations in this geometry. Under homeotropic surface anchoring conditions, the director organization shown in figure 4(*c*) is planar polar with two line defects in the cylinder-like region (*bc* cross-section) of the spheroid, with a radial configuration in the nearly hemispherical end-capping regions (*ac* and *ab* cross-sections). The observation of the planar polar configuration with two line defects in the cylinder-like region in the centre of the prolate spheroid is in excellent agreement with recent Monte Carlo simulations of liquid crystals confined to cylindrical domains using the Lebwohl–Lasher potential [21]. There it was shown that for small values of the cylinder radius, the planar polar configuration with two line defects was the stable arrangement. Iannacchione *et al.* [8] proposed a 'radial-like' structure for elongated ellipsoidal

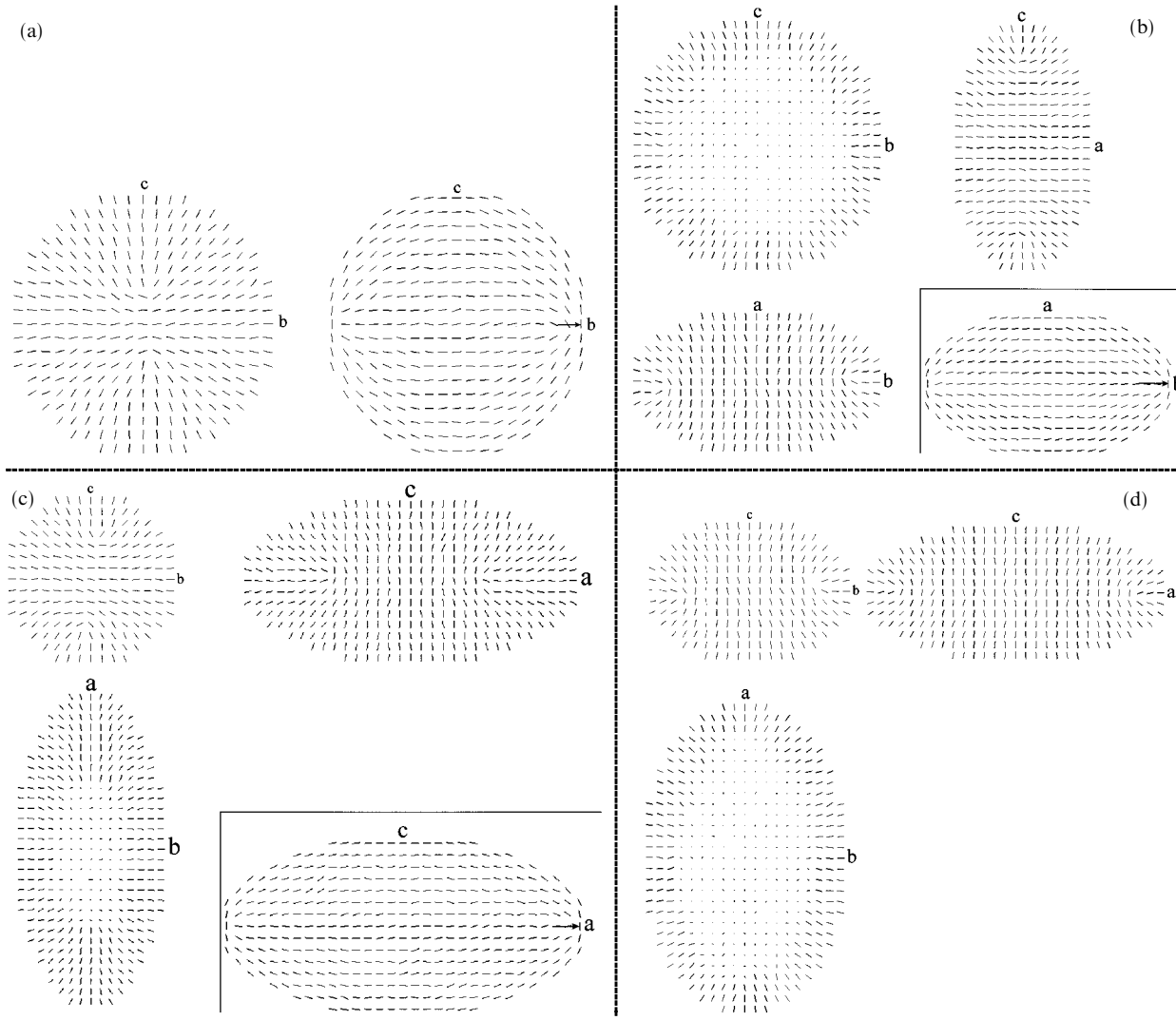

Figure 4. Director configuration for the four ellipsoidal cases studied at $T^* = 0.2$: (*a*) spherical ($19 \times 19 \times 19$), (*b*) oblate spheroid ($13 \times 23 \times 23$), (*c*) prolate spheroid ($31 \times 15 \times 15$) and (*d*) ellipsoid ($29 \times 19 \times 13$). The *cb* cross-section is shown in the spherical case. For the three ellipsoidal cases the configurations in the *cb*, *ca* and *ab* cross-sections are shown. Bipolar configuration is shown only for the spherical, oblate and prolate spheroid geometries. The arrows represent the direction of the bipolar symmetry axis.

droplets with homeotropic anchoring that comprised two half-point defects located at the foci and connected by a line segment defect stretching between the ellipsoid extrema. The former feature has been found here, but the line defect was not observed in any of the simulations performed in this study.

In the more general case of an ellipsoid ($a > b > c$), a direction of preferred orientation parallel to the minor axis (*c*) may be seen from figure 4 (*d*). The directors align themselves perpendicular to the direction along which the surface has the lowest curvature. Interestingly, the director configuration shows the line defect encircling the ellipsoid in the *ab* plane similar to that seen in the oblate spheroid case.

In the case of the bipolar configuration which involves tangential or planar orientation of the directors along a symmetry axis, the differences between the ellipsoidal and spherical domains is less evident visually. The bipolar configurations are shown in figures 4 (*a–c*) for the spherical, oblate and prolate spheroids respectively, with the bipolar symmetry axis oriented along the most preferred direction in each case. For oblate spheroids the bipolar symmetry axis lies in the plane formed by the two equal minor axes (*bc* plane) whereas for the prolate spheroid it lies along the major axis (*a*). The only discernible feature is the higher degree of parallel orientation among the directors in the prolate and oblate spheroids compared with that in the sphere, which is in

agreement with the analysis of the order parameter in figure 3.

3.3. *The effect of an external electric field*

With the model characterized, the response of ellipsoidal domains to an externally applied electric field can be examined. The case where the number of directors (volume) is held approximately constant, but the domain shape is varied between the four cases, is taken up first. Based on the above analysis, a very anisotropic response to applied fields is expected in the ellipsoidal domains. Therefore, the field was applied at different orientations with respect to the major axis (a) of the ellipsoid. In spherical coordinates, field directors were defined by varying the polar angle θ from 0° to 90° in 15° increments with the azimuthal angle ϕ held constant at 0°. This is of course all that is required in the case of the oblate and prolate spheroids, since the curvature is invariant with the azimuthal angle ϕ for a given θ. However, in the case of a general ellipsoid ($a \neq b \neq c$) the situation is more complex and the entire quadrant ($0° < \theta < 90°$; $0° < \phi < 90°$) would need to be explored in order fully to map out the effect of the surface curvature. The field order parameter (S_E) is calculated as

$$S_E = \frac{1}{2}\langle 3|\mathbf{n}_i \ \mathbf{n}_E|^2 - 1\rangle \tag{6}$$

where $\mathbf{n}_i$ represents the orientation of the nematic and $\mathbf{n}_E$ represents the direction of the applied field.

The dependence of the field order parameter S_E on the field strength and orientation for the prolate and oblate spheroids under homeotropic surface anchoring conditions at $T^* = 0.2$ is shown in figure 5. A schematic diagram illustrating the variation in the direction of electric field is also shown. As the magnitude of the electric field is increased, the expected increase in the order induced by the field (S_E) is seen. In all cases S_E shows a rapid increase with the electric field, attaining a value between 0.7–0.85 at $E = 0.5$. At $E = 2.0$, S_E is essentially saturated with a value of ~ 0.95 independent of the orientation at which the field was applied.

As the orientation of the applied field is varied as shown in figure 5, a very different behaviour is manifested in the oblate and prolate cases. As θ is varied from 0° (corresponding to the a direction) to 90° (corresponding

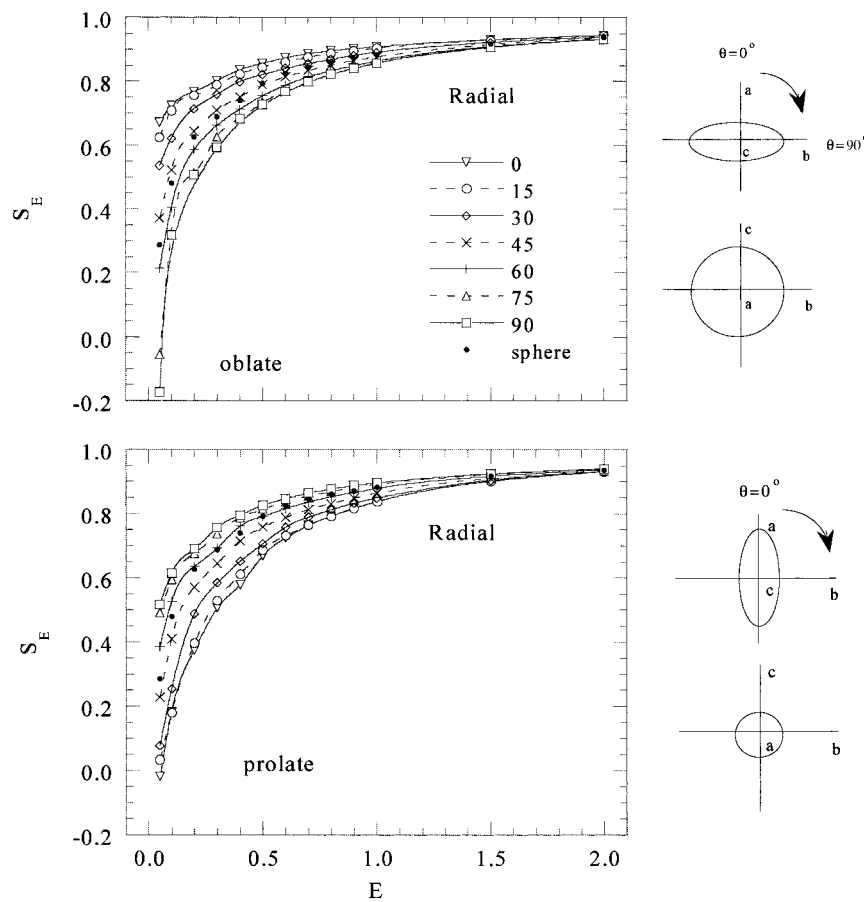

Figure 5. Variation of the field order parameter (S_E) as a function of applied field (E) for the oblate ($13 \times 23 \times 23$; 3841) and prolate ($31 \times 15 \times 15$; 3903) spheroids with homeotropic anchoring subjected to reorienting fields at different orientations to the major axis, as shown in the schematic diagrams at $T^* = 0.2$. Also shown are the results for the spherical case ($19 \times 19 \times 19$; 3887) denoted by filled circles. The curves are meant only as a guide to the eye.

to the b direction for $\phi = 0$) we see that S_E is displaced to progressively *lower* values for a given E in case of the oblate spheroid. This indicates that the ease of orientation is gradually decreasing as the field orientation is varied from 0° to 90°. This is in complete agreement with expectations based on the equilibrium director configurations shown in figure 4 (*b*). As seen from figure 4 (*b*) the directors possess an axial configuration with an encircling equatorial line defect perpendicular to the direction of preferred orientation. Therefore only a very small field applied at $\theta = 0°$ is required to bring about reorientation, since a majority of the directors are already pointed along the major axis. For comparison the results obtained for the spherical case have been overlaid on the plot. It can be seen that the directors in the oblate spheroid reorient more efficiently compared with the spherical domain for all $\theta < 45°$. Therefore we may conclude that directors confined to an oblate spheroid are most efficiently reoriented when the field is applied *parallel* to the major axis.

For the prolate case, the exact opposite behaviour ensues, that is as θ is varied from 0 to 90° S_E is displaced to progressively *higher* values for a given value of the applied field. Compared with the oblate case, the increase in S_E with E is more gradual. The S_E values for the prolate case for $\theta > 60°$ are higher than those for the

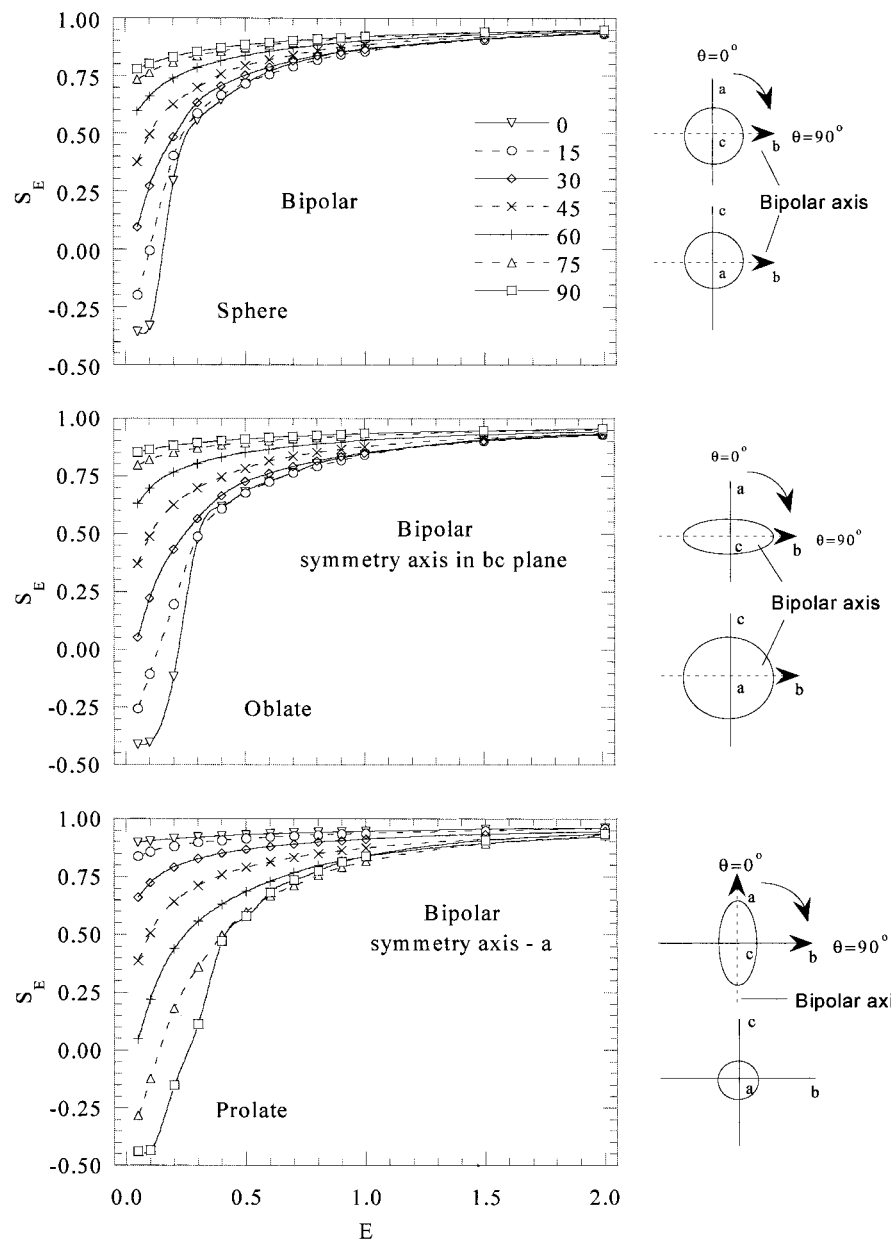

Figure 6. Dependence of the field order parameter (S_E) on the strength and orientation of the applied field for spherical, oblate and prolate spheroidal domains with bipolar configuration (homogeneous surface anchoring) at $T^* = 0.2$. The curves are meant only as a guide to the eye. The domain sizes are the same as in figure 5. The schematic diagrams show the orientation of the applied field with respect to the major axis of the ellipsoids and also the direction of the bipolar symmetry axis (broken curve with arrowhead).

spherical case at all E. Directors confined to prolate spheroids are most easily oriented when the field is applied *perpendicular* to the major axis. The fact that both prolate and oblate spheroids achieve a high degree of orientation at low field strengths is in excellent agreement with a host of experimental results [4–10] showing that PDLCs with ellipsoidal domains switch much faster and at lower switching voltages than do spherical domains. The results presented here can only confirm the latter experimental observations since there is no provision in the simulations to study time-dependent phenomena.

In figure 6 the dependence of the order parameter on the orientation of the applied field is shown for the spherical, oblate and prolate spheroid geometeries with bipolar configuration. As expected, S_E is the highest when the field is applied along the bipolar symmetry axis and lowest when applied perpendicular to the symmetry axis at a given field strength. A very large disparity in the values of S_E can be seen as θ is varied from 0° to 90°. No significant differences may be discerned in the behaviour of the different geometries, except that in the most favourable orientation, the prolate and oblate spheroids seem to orient more at a given field strength compared with the spherical domains. This is also as expected since the anisotropic domain shape stabilizes the bipolar symmetry axis along a particular direction, which lies along the major axis and in the plane formed by the minor axes, respectively, for prolate and oblate spheroids. Therefore under the above definition of the bipolar symmetry axis, oblate and prolate spheroids are most easily oriented when the field is applied *perpendicular* and *parallel* to the major axis, respectively.

On the basis of these results it is possible to predict the order of efficiency of reorientation with respect to the axes of the more general case of an ellipsoid. For $a > b > c$, we should observe $S_{Ec} > S_{Eb} > S_{Ea}$ at any given value of the applied field for domains with homeotropic surface anchoring and $S_{Ea} > S_{Eb} > S_{Ec}$ for homogeneous surface anchoring with the bipolar axis defined along a. The results for the ellipsoidal case are shown in figure 7 at $T^* = 0.2$ which is in accordance with these expectations. In fact for the bipolar case the trend is more aptly described as $S_{Ea} > S_{Eb} = S_{Ec}$. Therefore it is demonstrated rather conclusively that the ease of orientation of an elongated ellipsoid ($a > b > c$) is the highest when the field is applied along the minor axis (c) for radial and along the major axis (a) for the bipolar configuration.

Finally the effect of varying the oblate and prolate nature of the spheroids can be explored. For this the field was applied parallel and perpendicular to the major axis for the oblate and prolate spheroids, respectively, since these have already been determined to be the

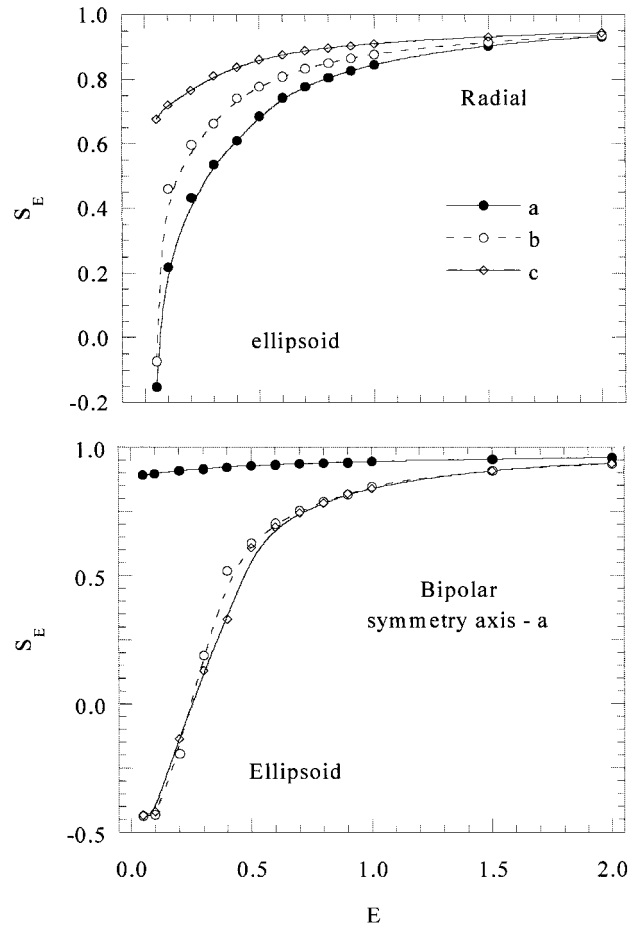

Figure 7. Comparison of reorientation of directors along different axes of an ellipsoidal droplet with both homeotropic and homogeneous anchoring ($29 \times 19 \times 13$) as a function of applied field at $T^* = 0.2$.

optimum orientations under homeotropic surface anchoring from the previous analysis. The results are shown in figure 8 where the 'oblateness' and 'prolateness' was varied until the spherical geometry was attained. S_E is shifted towards higher values at a given field as the 'oblateness' increases. The dependence of the response to an applied field is found to be pronounced in the case of the oblate spheroids over the entire range of field strengths studied. A similar behaviour, though to a lesser extent, is found in the case of the prolate spheroids. As the 'prolateness' is increased (the domain becomes more elongated) S_E is shifted towards higher values at a given field. However, in this case the size dependence of the response is evident only at low field strengths, with the behaviour becoming indistinguishable at high field strengths ($E > 0.5$). In both cases a spheroidal geometry is found to yield higher S_E values at a given E compared to the spherical case. This leads to a structure–property relationship to be established with respect to the most preferred geometry for the case of radial configuration with

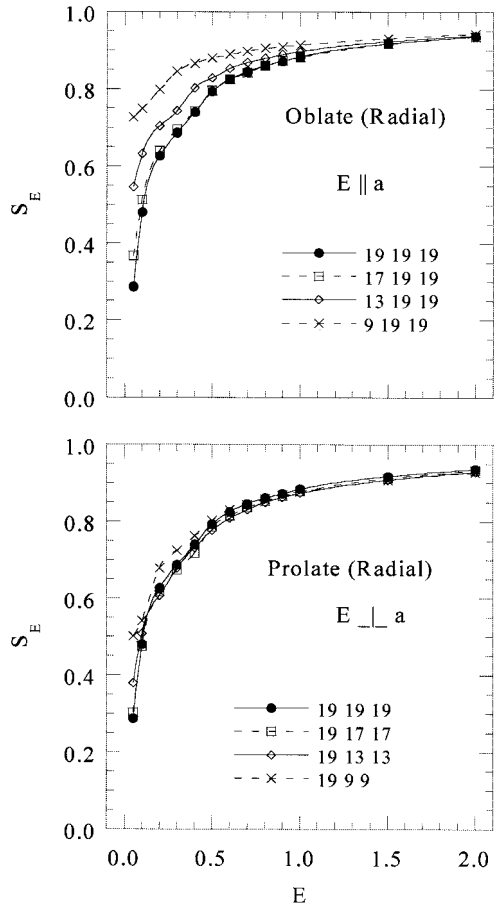

Figure 8. The effect of oblateness and prolateness of spheroids on the field order parameter as a function of applied field at $T^* = 0.2$ for homeotropic anchoring conditions. The field was applied perpendicular and parallel to the major axis for the oblate and prolate spheroids, respectively.

homeotropic surface anchoring. The ease of orientation, as defined by the attainment of high order at low field strengths, is found to increase as the ellipsoidal geometry is varied from spherical → prolate spheroidal → oblate spheroidal/elongated ellipsoidal in that order.

The effect of oblateness and prolateness for domains with bipolar configuration are shown in figure 9. Here the results are shown for two orientations of the applied field: parallel and perpendicular to the bipolar symmetry axis. As the oblateness or prolateness of the domain is increased, the ease of orientation also increases when the field is applied along the bipolar symmetry axis. This can be traced to the domains acquiring an axial configuration as the oblateness is increased. However, when the field is applied perpendicular to the bipolar axis, the behaviour reverses, with the ease of orientation decreasing as the oblateness or prolateness is increased. The response of bipolar droplets is therefore shown to be extremely sensitive to the orientation of the applied field.

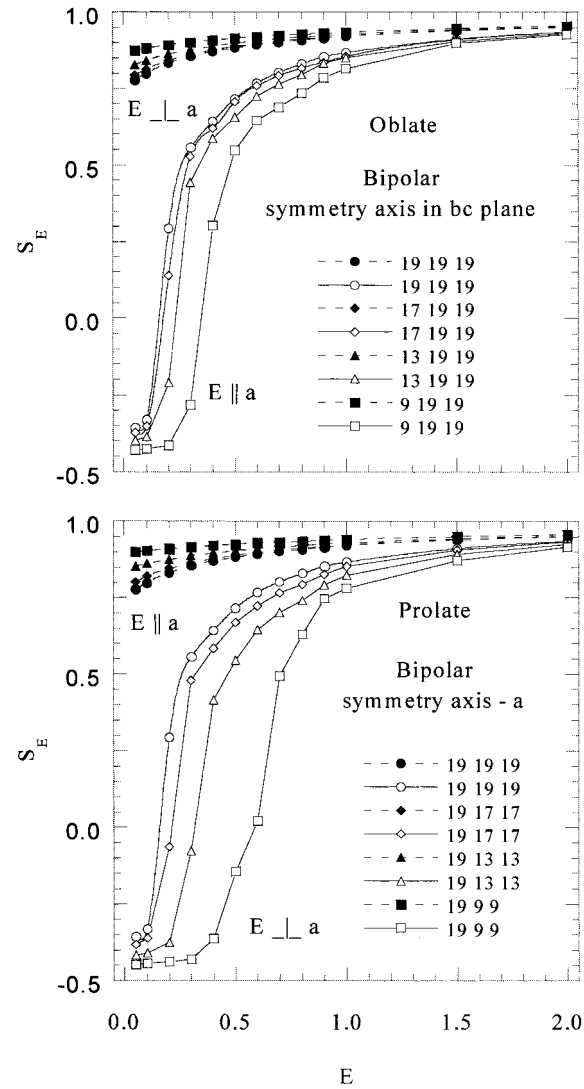

Figure 9. The effect of oblateness and prolateness of spheroids on the field order parameter as a function of applied field at $T^* = 0.2$ for homogeneous anchoring conditions. The field was applied parallel and perpendicular to the bipolar symmetry axis as shown.

4. Conclusions

Mesoscale modelling techniques have been used to predict the equilibrium properties, director configurations and effects of an applied electric field, for nematic liquid crystals confined to ellipsoidal domains with homeotropic and homogeneous surface anchoring. We show that under equilibrium conditions, homeotropic surface anchoring leads to very different director configurations in nematics confined to ellipsoidal and spherical domains. The directors within the spherical domain exhibit a radial configuration. The directors confined to oblate spheroids ($a < b = c$) and elongated ellipsoids ($a > b > c$) possess an axial configuration with an equatorial line

defect encircling the spheroid/ellipsoid perpendicular to the direction of preferred orientation. Prolate spheroids ($a > b = c$) possess the planar polar configuration with two line defects in the cylinder-like region, end-capped by two nearly hemispherical regions with the radial configuration. Homogeneous surface anchoring leads to nearly identical bipolar configuration in all cases with the extent of parallel orientation showing a slight increase in the case of elongated ellipsoids and prolate spheroids.

Under the influence of an externally applied field, the ellipsoidal domains are shown to have a very different behaviour. It is demonstrated that oblate spheroids with homeotropic surface anchoring are most easily reoriented when the field is applied parallel to the major axis (a), whereas the prolate spheroids are most readily oriented when the field is applied perpendicular to the major axis. For the bipolar configuration (homogeneous anchoring) the ease of orientation is highest when the field is applied along the bipolar axis. We find that among the spherical, oblate spheroidal, prolate spheroidal and elongated ellipsoidal confinement geometries, the elongated ellipsoids and oblate spheroids are the most efficient (achieving a higher degree of orientation at a given field) followed by the prolate spheroids and spheres under homeotropic surface anchoring. For domains involving the bipolar configuration (homogeneous surface anchoring) elongated ellipsoids and prolate spheroids are shown to be the most efficient confinement geometries.

We are indebted to the Materials and Manufacturing Directorate at the Air Force Research Laboratory for financial support of this work. The authors wish to acknowledge the efforts of Mr Jacque Henes (University of Dayton Research Institute) in managing the computational facilities. B.L.F. gratefully acknowledges the generous hospitality of A. Windle and his colleagues during a sabbatical supported in part by an ESRF grant and the University of Virginia.

References

[1] Doane, J. W., 1990, in *Liquid Crystals; Applications and Uses*, edited by Bahadur, B. (Singapore: World Scientific).
[2] Drzaic, P. S., 1995, *Liquid Crystal Dispersions* (Singapore: World Scientific).
[3] Klosowicz, S. J., 1996, *Opto-Electron. Rev.*, **4,** 62.
[4] Sutherland, R. L., Natarajan, L. V., Tondiglia, V. P., Bunning, T. J., and Adams, W. W., 1995, *Proc. SPIE*, **2532,** 309.
[5] Bunning, T. J., Natarajan, L. V., Tondiglia, V. P., Sutherland, R. L., Vezie, D. L., and Adams, W. W., 1996, *Polymer*, **37,** 3147.
[6] Bunning, T. J., Natarajan, L. V., Tondiglia, V. P., Sutherland, R. L., Vezie, D. L., and Adams, W. W., 1995, *Polymer*, **36,** 2699.
[7] Bunning, T. J., Natarajan, L. V., Tondiglia, V. P., Dougherty, G., and Sutherland, R. L., 1997, *J. polym. Sci: polym. Phys.*, **35,** 2825.
[8] Iannacchione, G. S., Finotello, D., Natarajan, L. V., Sutherland, R. L., Tondiglia, V. P., Bunning, T. J., and Adams, W. W., 1996, *Europhys. Lett.*, **36,** 425.
[9] Huang, Z., Chidichimo, G., and Golemme, A., 1988, *Mol. Cryst. liq. Cryst.*, **312,** 165.
[10] Wu, B. G., Erdmann, J. H., and Doane, J. W., 1989, *Liq. Cryst.*, **5,** 1453.
[11] Metropolis, N., Rosenbluth, A. W., Rosenbluth, M. N., Teller, A. H., and Teller, E., 1953, *J. chem. Phys.*, **21,** 1087.
[12] Lebwohl, P. A., and Lasher, G., 1972, *Phys. Rev. A*, **6,** 426.
[13] Fabbri, U., and Zannoni, C., 1986, *Mol. Phys.*, **58,** 763.
[14] Zannoni, C., 1986, *J. chem. Phys.*, **84,** 424.
[15] Chiccoli, C., Pasini, P., Semeria, F., and Zannoni, C., 1990, *Phys. Lett. A*, **150,** 311.
[16] Chiccoli, C., Pasini, P., Semeria, F., and Zannoni, C., 1992, *Mol. Cryst. liq. Cryst.*, **212,** 197.
[17] Chiccoli, C., Pasini, P., Semeria, F., and Zannoni, C., 1992, *Mol. Cryst. liq. Cryst.*, **221,** 19.
[18] Chiccoli, C., Pasini, P., Semeria, F., Berggren, E., and Zannoni, C., 1995, *Mol. Cryst. liq. Cryst.*, **266,** 241.
[19] Kilian, A., 1993, *Liq. Cryst.*, **14,** 1189.
[20] Chiccoli, C., Pasini, P., Semeria, F., Berggren, E., and Zannoni, C., 1996, *Mol. Cryst. liq. Cryst.*, **290,** 237.
[21] Smondyrev, A. M., and Pelcovits, R. A., 1999, *Liq. Cryst.*, **26,** 235.
[22] Bellini, T., Chicolli, C., Pasini, P., and Zannoni, C., 1996, *Mol. Cryst. liq. Cryst.*, **290,** 227.
[23] Bellini, T., Chicolli, C., Pasini, P., and Zannoni, C., 1996, *Phys. Rev. E*, **54,** 2647.
[24] Zhu, J., Ding, J., Lu, J., and Yang, Y., 1998, *Polymer*, **39,** 6455.
[25] Bedford, S. E., Nicholson, T. M., and Windle, A. H., 1991, *Liq. Cryst.*, **10,** 63.
[26] Hobdell, J. R., and Windle, A. H., 1995, *J. chem. Soc. Faraday Trans.*, **91,** 2497.
[27] Berggren, E. Zannoni, C., Chiccoli, C., Pasini, P., and Semeria, F., 1993, *Phys. Rev. E*, **49,** 614.
[28] Berggren, E., Zannoni, C., Chiccoli, C., Pasini, P., and Semeria, F., 1992, *Chem. Phys. Lett.*, **197,** 224.
[29] Chiccoli, C., Pasini, P., Semeria, F., and Zannoni, C., 1993, *Phys. Lett. A*, **176,** 428.
[30] Allen, M. P., and Tildesley, D. J., 1987, *Computer Simulations of Liquids* (Oxford: Clarendon).
[31] Golemme, A., Zumer, S., Allender, D. W., and Doane, J. W., 1988, *Phys. Rev. Lett.*, **61,** 2937.
[32] Iannacchione, G. S., and Finotello, D., 1992, *Phys. Rev. Lett.*, **69,** 2094.
[33] Iannacchione, G. S., Crawford, G. P., Doane, J. W., and Finotello, D., 1992, *Mol. Cryst. liq. Cryst.*, **222,** 205.